



Excessive Glucocorticoids During Pregnancy Impair Fetal Brown Fat Development and Predispose Offspring to Metabolic Dysfunctions

Yan-Ting Chen,¹ Yun Hu,¹ Qi-Yuan Yang,¹ Jun Seok Son,¹ Xiang-Dong Liu,¹ Jeanene M. de Avila,¹ Mei-Jun Zhu,² and Min Du¹

Diabetes 2020;69:1662–1674 | <https://doi.org/10.2337/db20-0009>

Maternal stress during pregnancy exposes fetuses to hyperglucocorticoids, which increases the risk of metabolic dysfunctions in offspring. Despite being a key tissue for maintaining metabolic health, the impacts of maternal excessive glucocorticoids (GC) on fetal brown adipose tissue (BAT) development and its long-term thermogenesis and energy expenditure remain unexamined. For testing, pregnant mice were administered dexamethasone (DEX), a synthetic GC, in the last trimester of gestation, when BAT development is the most active. DEX offspring had glucose, insulin resistance, and adiposity and also displayed cold sensitivity following cold exposure. In BAT of DEX offspring, *Ppargc1a* expression was suppressed, together with reduced mitochondrial density, and the brown progenitor cells sorted from offspring BAT demonstrated attenuated brown adipogenic capacity. Increased DNA methylation in *Ppargc1a* promoter had a fetal origin; elevated DNA methylation was also detected in neonatal BAT and brown progenitors. Mechanistically, fetal GC exposure increased GC receptor/DNMT3b complex in binding to the *Ppargc1a* promoter, potentially driving its de novo DNA methylation and transcriptional silencing, which impaired fetal BAT development. In summary, maternal GC exposure during pregnancy increases DNA methylation in the *Ppargc1a* promoter, which epigenetically impairs BAT thermogenesis and energy expenditure, predisposing offspring to metabolic dysfunctions.

Stress, including anxiety and depression, has become a serious health concern in women during pregnancy (1,2). National population-based studies reported that 15.2%

of pregnant women have anxiety disorder and 37% and 17% of pregnant women have depressive symptoms and severe depressive disorders, respectively (1,2). Glucocorticoids (GC) are major hormones responsive to stress, and the maternal stress during pregnancy significantly increases fetal exposure to GC (3,4). The activity of 11 β -hydroxysteroid dehydrogenase, an enzyme limiting maternal GC across the placental barrier, was also reduced by maternal stress (5), further exaggerating excessive exposure of fetuses to GC (6,7).

Programming effects of hyper-intrauterine GC increase susceptibility of offspring to not only neurophysiological and psychological disorders but also the risk of childhood and adult obesity (8–11). Overweight and obesity, due to excessive accumulation of white adipose tissue, are closely associated with type 2 diabetes, cardiovascular diseases, and several cancers (12,13). Different from white adipose tissue, brown adipose tissue (BAT) dissipates energy through thermogenic activity of uncoupling protein 1 (UCP-1), preventing obesity and type 2 diabetes (12–14). Mitochondria are key organelles in maintaining BAT thermogenic functions and energy expenditure, and UCP-1 is anchored in inner mitochondrial membrane (12–14). Peroxisome proliferator-activated receptor γ coactivator-1 α (*Ppargc1a*) (protein PGC-1 α) is a master regulator of mitochondrial biogenesis (15,16), and its transcriptional inhibition decreases mitochondrial density and UCP-1 protein, contributing to cold sensitivity and obesity (17). Recently, hyper-DNA methylations have been identified in the *Ppargc1a* promoter in pancreas (18) and skeletal muscle (19) of patients with type 2 diabetes. Adiposity, glucose

¹Nutrigenomics and Growth Biology Laboratory, Department of Animal Sciences, Washington State University, Pullman, WA

²School of Food Sciences, Washington State University, Pullman, WA

Corresponding author: Min Du, min.du@wsu.edu

Received 3 January 2020 and accepted 6 May 2020

This article contains supplementary material online at <https://doi.org/10.2337/figshare.12252863>.

© 2020 by the American Diabetes Association. Readers may use this article as long as the work is properly cited, the use is educational and not for profit, and the work is not altered. More information is available at <https://www.diabetesjournals.org/content/license>.

tolerance, and insulin resistance induce epigenetic modulations, which reduce *Ppargc1a* expression and mitochondrial biogenesis across tissues (18,19). Currently, little information is available on changes and functional roles of *Ppargc1a* promoter DNA methylation in BAT function of obese and diabetic mice or humans with obesity and diabetes. Because of the BAT importance in energy expenditure and glucose homeostasis (12,13), revealing the link between offspring BAT phenotypes and DNA methylation of *Ppargc1a* promoter in responding to maternal hyper-GC during pregnancy is of key interest.

Previous evidence suggests that excessive GC in circulation increase the risks of obesity in adult mice (20). Similarly, patients with Cushing syndrome, due to chronic hypercortisolism, are also characterized with insulin resistance and central obesity (20). Hyper-GC were reported to inhibit BAT thermogenesis, but a recent study reversibly showed that excessive GC activate human BAT thermogenic activity (21). The inconsistency in reports underscores the knowledge deficiency in the direct GC exposure on adult BAT thermogenesis. Moreover, the effects of maternal hyper-GC exposure during pregnancy on fetal BAT development and long-term energy expenditure and thermogenesis in adult offspring remain unexamined. In this study, pregnant mice were administered with synthetic GC dexamethasone (DEX) during the last trimester; synthetic GC can readily cross the placenta, imitating maternal stress-induced fetal hyper-GC exposure as previously reported (22–24). In addition, DEX injection is used for >70% of women at risk of preterm delivering (25). The development of BAT is initiated around mid-gestation and followed by rapid brown adipogenic differentiation in the last trimester (12,13). Targeting this most active stage of brown adipogenesis (12–14), we hypothesized that the intrauterine hyper-GC exposure has substantial impacts on fetal BAT development, leading to changes of postnatal developmental trajectory and functions. We further hypothesized that maternal hyper-GC exposure epigenetically inhibits *Ppargc1a* expression, persistently reducing its expression and BAT energy expenditure and thermogenesis in offspring.

RESEARCH DESIGN AND METHODS

Animal Studies

Wild-type female C57BL/6J mice (The Jackson Laboratory, Bar Harbor, ME) at 4 months of age were mated with wild-type male mice fed a regular diet (10% energy from fat, D12450H; Research Diets, New Brunswick, NJ). Successful mating was determined by the presence of a copulation plug in the vagina and marked as embryonic day 0.5 (E0.5). At E14.5, pregnant mice were randomly separated into two groups intraperitoneally administered with PBS (as control) or 0.1 mg/kg body wt DEX (D4902; Sigma-Aldrich) daily until E20.5. After birth, the litter size was standardized to six and the maternal mice together with their offspring were housed at room temperature (22°C) until weaning (postnatal day 21 [P21]). After weaning,

male offspring in control and DEX groups were further randomly assigned to a chow (10% energy from fat) or obesogenic (high-fat diet [HFD]) (60% energy from fat; D12492) diet until 4 months of age. At 4 months old, a portion of offspring were acclimated to thermoneutrality (30°C) for 4 weeks to examine BAT-independent thermogenic changes due to maternal DEX exposure (26–28). At P0, P21, and 4 months, offspring were euthanized by CO₂ and brown fat (BAT) was collected for analyses. Due to the small size of neonatal BAT, neonates from the same litter were pooled. Each dam (each pregnancy) was treated as an experimental unit. All animal studies were conducted in a Washington State University animal facility accredited by the Association for Assessment and Accreditation of Laboratory Animal Care. Animal protocol was approved by the Washington State University Institute of Animal Care and Use Committee.

Flow Cytometry Sorting (FACS)

FACS was performed as previously described (14). BAT was digested in 0.2% collagenase type II (285 units/mg) in DMEM-free FBS medium for 30 min at 37°C. Tissues debris was filtered through 40- μ m strainers, and the filter solution was centrifuged at 400g for 5 min. After centrifugation, BAT stromal vascular fractions were blocked in 1% BSA for 15 min on ice. Cells were washed by PBS and incubated in conjugated CD45 (phycoerythrin/Cy7; BioLegend) and PDGFR α (allophycocyanin; BioLegend) in the dark at 4°C for 1 h. Cells were washed with PBS and sorted in a SY3200 Cell Sorter (Sony Biotechnology, San Jose, CA). Flow cytometry data were analyzed using FlowJo software (Treestar). Gates were established using fluorescence minus controls.

DNA Methylation Immunoprecipitation

DNA Methylation Immunoprecipitation (MeDIP) analysis was performed as previously described (14). BAT was digested in protease K solution. Total DNA was isolated from solution containing Tris-phenol, chloroform, and isoamyl alcohol. Isolated DNA was dissolved into Tris-EDTA buffer followed by sonication (30% power, 10 s on/off for 5 min) on ice. Average 300–500 base pair DNA fragment size was obtained and verified by electrophoresis in 2% agarose gel. Denatured DNA (2 mg) containing RNase A was incubated with 2 μ g antibody against 5-methylcytosine (5mC) (Zymo Research, Irvine, CA) or anti-mouse IgG (Thermo Fisher Scientific) overnight at 4°C. The DNA-antibody solution was further incubated with precleaned protein A magnetic beads (Cell Signaling Technology) at 4°C for 1 h. Washed beads were incubated in digestion buffer to recover precipitated DNA at 65°C for 3 h. Recovered DNA was quantified by quantitative PCR (qPCR). Primers for MeDIP qPCR are listed in Supplementary Table 1.

Bisulfite Pyrosequencing

Genomic DNA was converted by bisulfite using EZ DNA Methylation-Direct Kit (D5021; Zymo Research). Converted

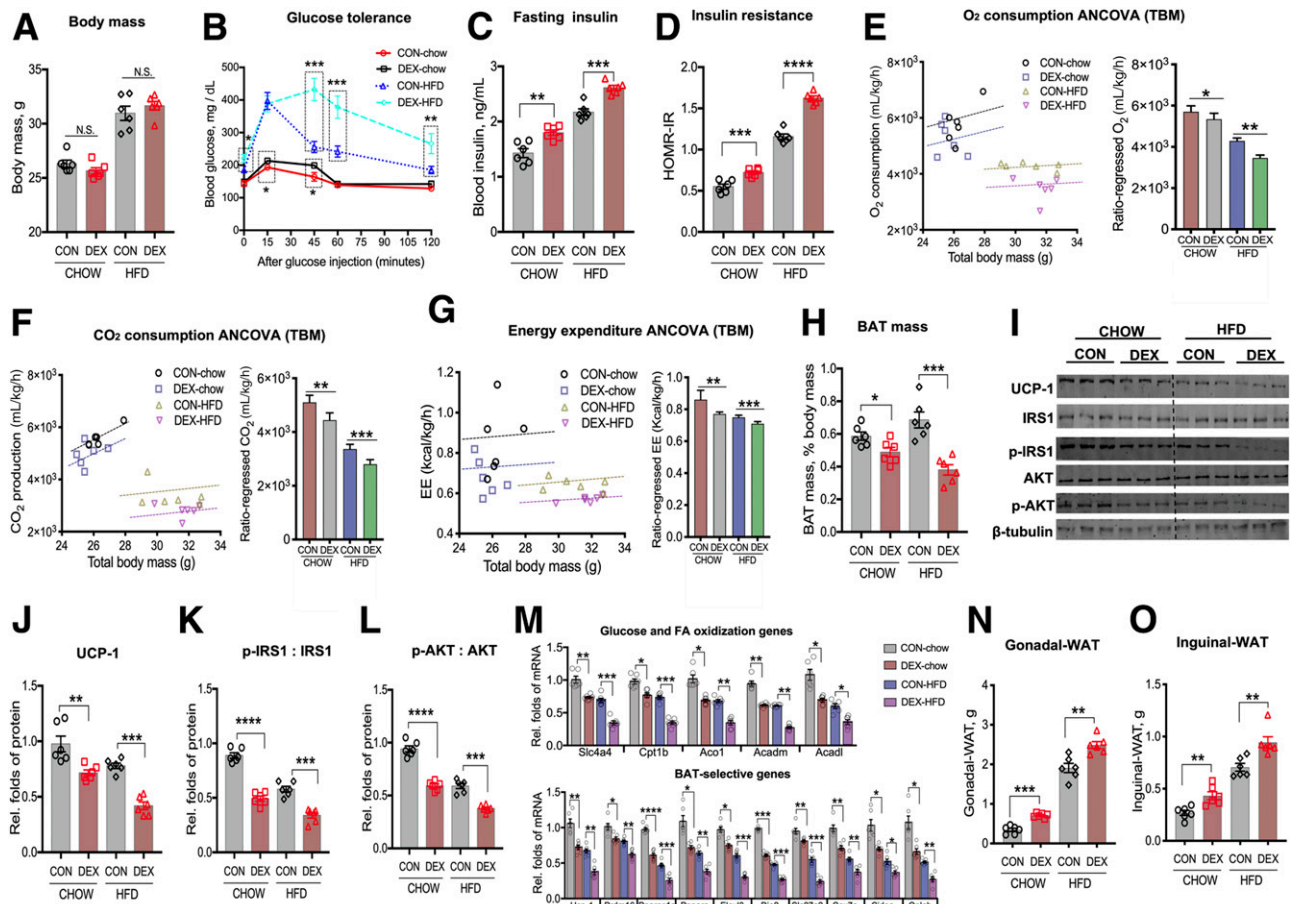


Figure 1—Maternal DEX administration decreases BAT energy expenditure, contributing to offspring metabolic dysfunctions and obesity at room temperature (22°C). A–G: Data were collected in offspring fed with chow or HFD until 4 months of age. A: Body mass of offspring at 4 months of age ($n = 6$ per group). After 6 h of fasting, glucose tolerance test (B), insulin in serum (C), and insulin resistance (HOMA of IR [HOMA-IR]) (D) were measured in offspring fed chow or HFD ($n = 6$ per group). In metabolic analyses, volumes of oxygen consumption (E), CO₂ respiration (F), and energy expenditure (G) were measured in offspring fed chow or HFD. Metabolic data were regressed to total body mass (TBM) ($n = 6$ per group). H–M: Intrascapular BAT was collected in offspring at 4 months of age fed with chow or HFD. H: BAT mass (% body mass) in offspring at 4 months of age ($n = 6$ per group). I: Representative images of immunoblotting measuring UCP-1 expression and total and phosphorylation (p-) of IRS1 (T612) and AKT (S473) in offspring BAT. Quantified protein contents of UCP-1 (J), ratio of phosphorylated IRS1 to total IRS1 (K), and phosphorylated AKT to total AKT (L) in offspring BAT. β-Tubulin was used as a loading control ($n = 6$ per group). M: Gene expressions in glucose uptake and fatty acid oxidation in offspring BAT. mRNA expression was normalized to 18S rRNA ($n = 6$ per group). N–O: Gonadal (N) and inguinal (O) fat mass in offspring fed chow or HFD at 4 months of age ($n = 6$ per group). Data are means ± SEM, and each dot represents one replicate (one pregnancy). * $P < 0.05$, ** $P < 0.01$, *** $P < 0.001$, **** $P < 0.0001$; unpaired one-way ANOVA (multiple tests) was used in analyses. CON, control; EE, energy expenditure; Rel., relative; WAT, white adipose tissue.

Insulin Resistance Test

After 6 h of fasting, insulin was measured using a mouse insulin ELISA (ALPCO). Insulin resistance was calculated according to the following formula: HOMA of insulin resistance = (fasting blood glucose mg/dL × 0.055) × (fasting insulin μU/mL)/22.5.

DEX Suppression Test

For assessment of hypothalamic-pituitary-adrenal axis activity, offspring at 4 months of age were intraperitoneally administrated with DEX (20 μg/kg) and blood was collected after 2 h. Corticosterone concentration in serum was measured with an ELISA kit (ADI-900; Enzo Life Sciences, Farmingdale, NY) according to the manufacturer’s instructions.

MTT Assay

Cells were incubated with 6 mg/mL 3-[4,5-dimethylthiazol-2-yl]-2,5-diphenyltetrazolium bromide (MTT) (Sigma-Aldrich) for 4 h. Formazan was dissolved in 100 μL DMSO, and the absorbance was measured at 540 nm using a microplate reader.

BrdU Proliferation Assay

Cells were incubated in 1 μmol/L BrdU (Sigma-Aldrich) for 24 h followed by BrdU (Cell Signaling Technology) immunostaining.

Statistical Analyses

Results were presented as means ± SEM. All statistical analyses were performed using SAS, version 9.4 (SAS

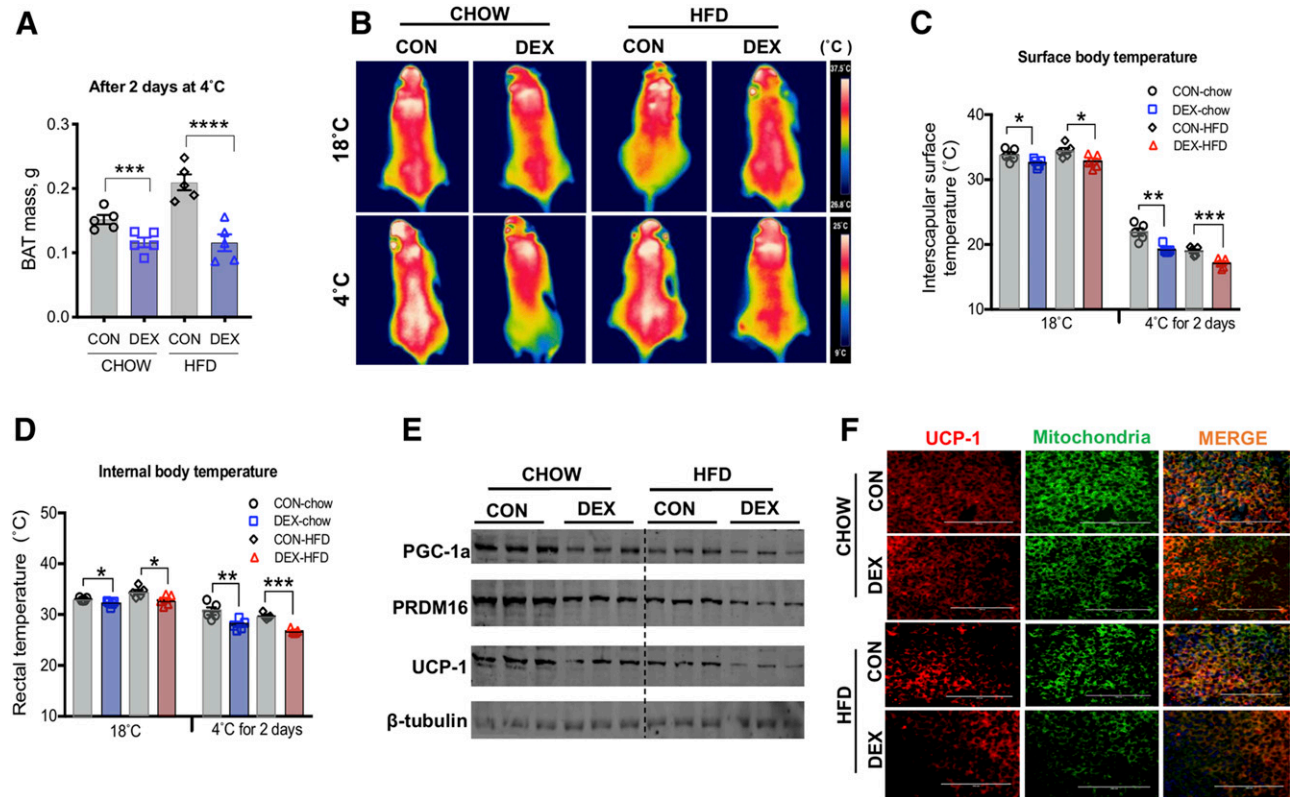


Figure 2—Maternal DEX administration decreases offspring BAT thermogenesis and increases cold sensitivity under cold challenge. *A–D*: At 4 months old, offspring fed with chow or HFD were exposed to 4°C for 2 days. *A*: BAT mass of offspring after cold challenge. *B*: Thermal imaging of surface temperature at interscapular region of offspring before and after cold challenge. Quantified surface temperature (*C*) and rectal temperature (*D*) in offspring fed chow or HFD before and after cold challenge ($n = 5$ per group). *E*: After 2 days of cold challenge, BAT of offspring fed chow or HFD was collected for immunoblotting analyses. β -Tubulin was used as a loading control ($n = 5$ per group). *F*: Immunohistochemical staining of UCP-1 and mitochondria in BAT of offspring fed chow or HFD after cold challenge. Scale bars, 100 μ m. Data are means \pm SEM, and each dot represents one replicate (litter). * $P < 0.05$, ** $P < 0.01$, *** $P < 0.001$; unpaired one-way ANOVA (multiple tests) was used in analyses. CON, control.

Institute, Cary, NC). Unpaired two-tail Student *t* test was applied for two-group comparison. One-way ANOVA was used in comparisons for multiple groups. Each dam (pregnancy) was used as an individual replicate. Metabolic chamber data were analyzed by National Institute of Diabetes and Digestive and Kidney Diseases minimal-change chronic pancreatitis ANCOVA multiple linear regression models (30,31). Significant differences are shown in figures as $P < 0.05$, $P < 0.01$, $P < 0.001$, and $P < 0.0001$.

Data and Resource Availability

The data sets generated and analyzed during this study are available from the corresponding author upon reasonable request.

RESULTS

Maternal GC Renders Metabolic Dysfunctions and Cold Sensitivity in Offspring

Pregnant mice were intraperitoneally administered with DEX during the last trimester of pregnancy, and DEX-treated maternal mice displayed similar food intake, body weight, and blood glucose compared with placebo mice at

room temperature (22°C) (Supplementary Fig. 1A–C). Regardless of feeding with chow or HFD, DEX offspring at 4 months of age had similar calorie intake and body mass (Fig. 1A and Supplementary Fig. 1D) but showed higher glucose tolerance, fasting insulinemia, and reduced insulin sensitivity compared with control offspring (Fig. 1B–D and Supplementary Fig. 1E). Metabolically, the use of ANCOVA with total body mass or lean mass as a covariate revealed that DEX offspring robustly exhibited lower O_2 consumption, CO_2 respiration, and energy expenditure (30,31) (Fig. 1E–G and Supplementary Fig. 1F–N). The difference of energy expenditure between control and DEX offspring was exaggerated when body fat effects were accounted for (Fig. 1E–G and Supplementary Fig. 1J–N), showing presence of metabolic dysfunctions in thermogenic fat. Consistently, DEX offspring had lower BAT mass (Fig. 1H) and thermogenic protein UCP-1 content (Fig. 1I and J), indicating blocked thermogenic function. In agreement with the hyperinsulinemia, BAT of DEX offspring had impaired insulin signaling as indicated by the reduced tyrosine phosphorylation of IRS-1 (T612) and serine phosphorylation of AKT (S473) (Fig. 1I, K, and L). Such reduction was

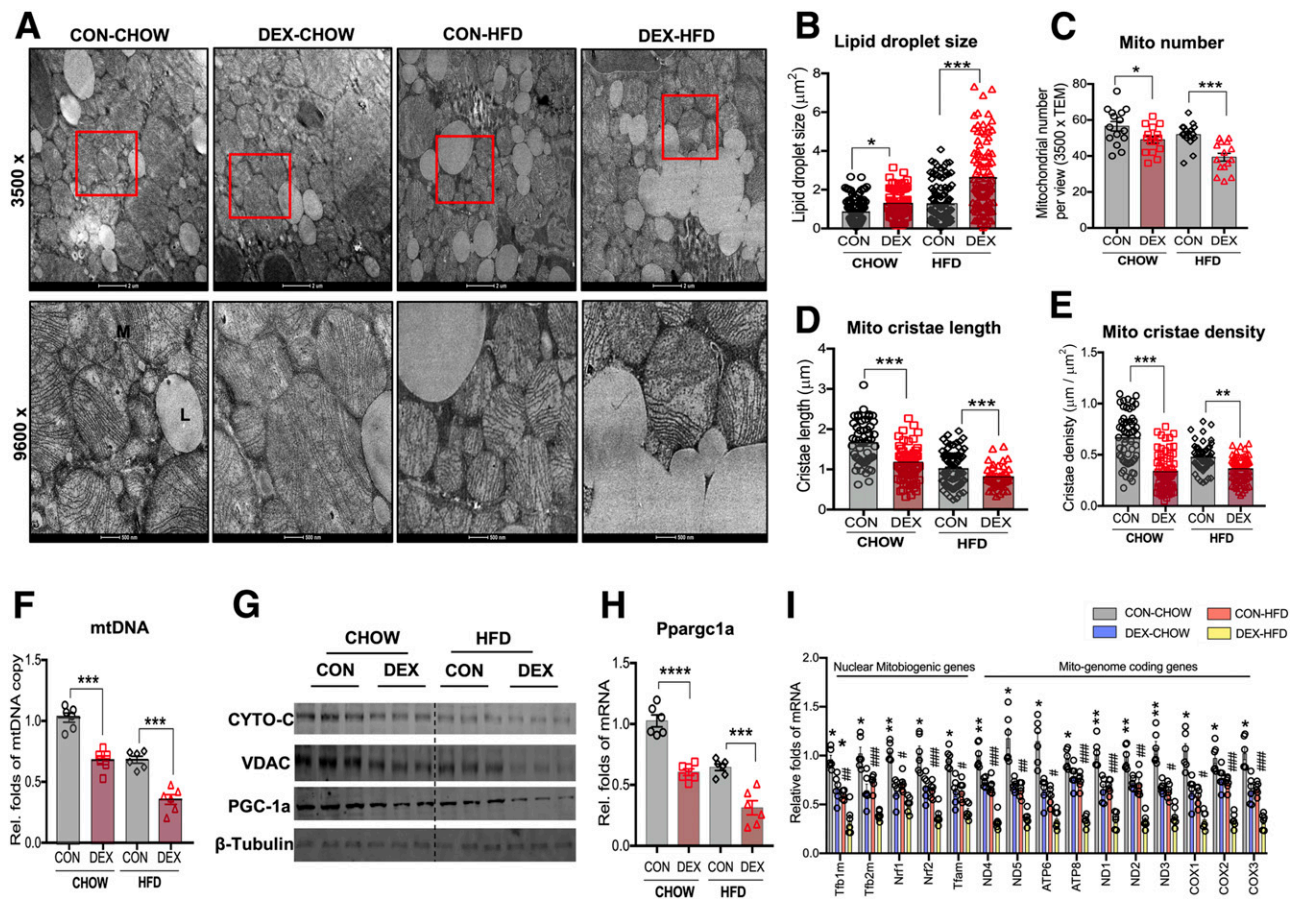


Figure 3—Maternal DEX administration inhibits *Pparg1a* expression and mitochondrial biogenesis in BAT of offspring at 4 months old. **A–E**: In TEM imaging, BAT of offspring fed chow or HFD was analyzed (**A**) followed by quantifications of lipid droplet size (**B**), mitochondria (Mito) number (**C**), and mitochondrial cristae length (**D**) and density (**E**). (Scale bar, ×3,500 for 2 µm, ×9,600 for 500 nm.) **F**: mtDNA copy number in offspring BAT. Amplification of mitochondrial genes was standardized to 18s rRNA and GAPDH ($n = 6$ per group). **G**: Immunoblotting in measuring mitochondrial biomass proteins: CYTO-C, VDAC, and master regulator protein PGC-1a. β-Tubulin was used as a loading control ($n = 6$ per group). **H**: mRNA expression of *Pparg1a* in BAT of offspring fed chow or HFD. Expression was normalized to 18S rRNA ($n = 6$). **I**: Gene expression of *Pparg1a* and downstream mitochondrial biogenic genes in nucleus and mitochondria encoded genes for oxidative phosphorylation and respiration chain in offspring BAT. Expression was normalized to 18S rRNA ($n = 6$ per group). Data are means ± SEM, and each dot represents one replicate (litter). * $P < 0.05$, ** $P < 0.01$, *** $P < 0.001$, **** $P < 0.0001$; unpaired one-way ANOVA (multiple tests) was used in analyses. CON, control; Rel., relative.

further confirmed following insulin stimulation (Supplementary Fig. 2A). Maternal GC exposure also decreased expression of genes involved in fatty acid oxidation and BAT thermogenesis in offspring BAT (Fig. 1M). The reduced energy expenditure and fatty acid oxidation in BAT contributed to lipid accumulation in gonadal and inguinal fat and increased total fat mass in DEX offspring regardless of chow or HFD feeding (Fig. 1N and O and Supplementary Fig. 2B). Moreover, muscle mass tended to be lower in DEX offspring, which was exacerbated by HFD feeding (Supplementary Fig. 2C and D).

To further test the mediatory roles of BAT thermogenesis in energy metabolic dysfunctions of DEX offspring, we acclimated offspring to thermoneutrality (30°C) to block BAT thermogenic activation (26–28). Consistent with previous reports (26–28), thermoneutrality blunted BAT activation as indicated by similar UCP-1 protein content between control and DEX offspring (Supplementary

Fig. 3A). No significant difference was observed for calorie intake and body mass (Supplementary Fig. 3B and C), but the difference in glucose, insulin sensitivity, and energy expenditure between control and DEX offspring was ameliorated under thermoneutrality (Supplementary Fig. 3D–L), showing that BAT thermogenic inactivation mediates metabolic dysfunctions in DEX offspring observed at room temperature.

After offspring were subjected to cold challenge (4°C) for 2 days, the difference of BAT mass became even greater between control and DEX offspring receiving either chow or HFD (Fig. 2A), showing the reduced BAT thermogenic plasticity. DEX offspring also had lower interscapular surface and core body temperatures (Fig. 2B–D), which were in agreement with inactivation of brown adipogenic and thermogenic proteins, including PGC-1a, PRDM16, and UCP-1 (Fig. 2E and Supplementary Fig. 4A–C). Accordingly, the mitochondrial density was also reduced due

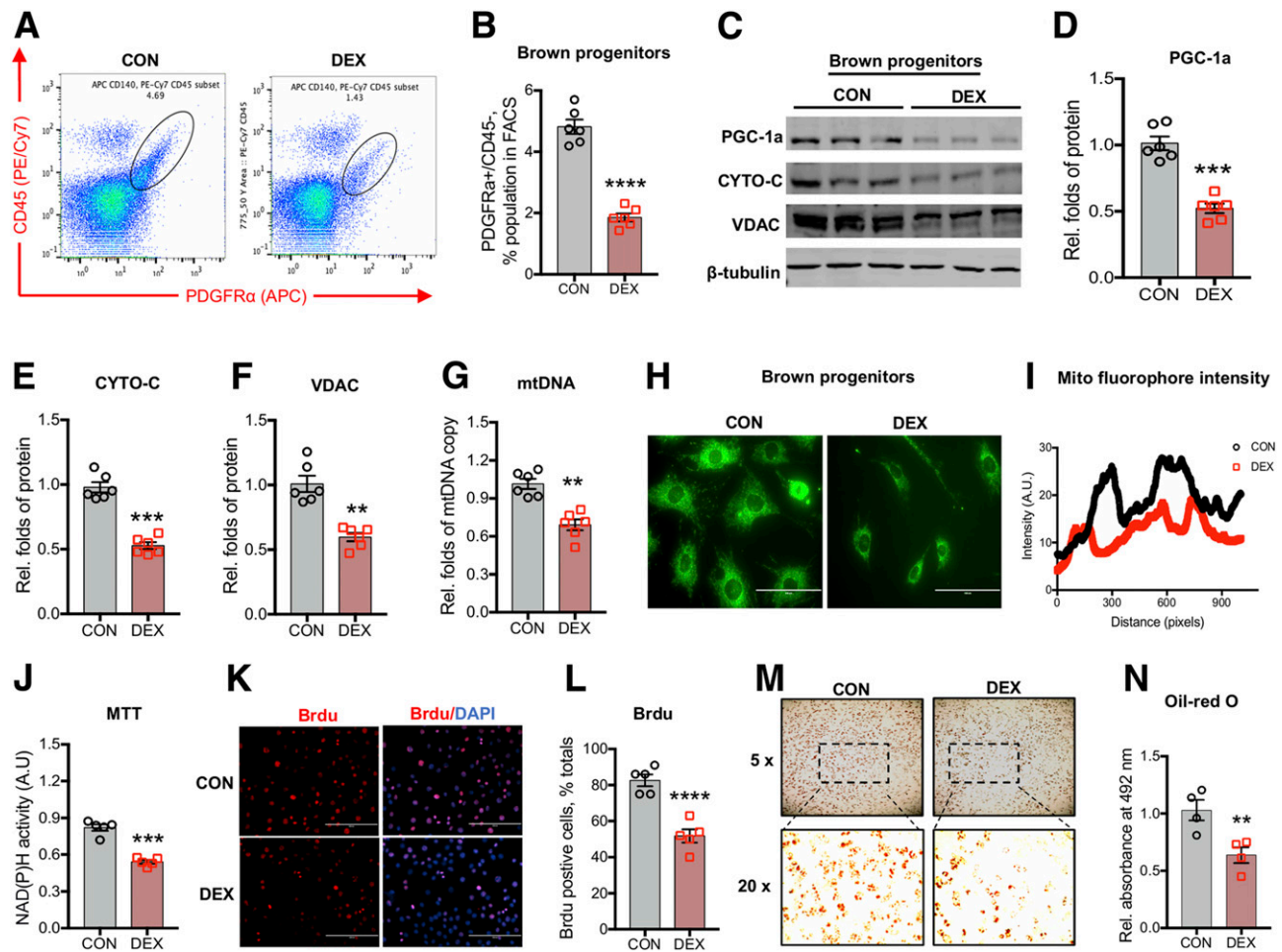


Figure 4—Maternal DEX administration inhibits *Pparg1a* expression and mitochondrial biogenesis of brown progenitors in offspring BAT at 4 months of age. **A** and **B**: Flow cytometry analyses (FACS) in sorting and measuring the population of brown progenitors in offspring BAT using brown progenitor markers $\text{Lin}^- \text{CD45}^-/\text{PDGFR}\alpha^+$ (also named as CD140). Positive population of brown progenitors shown in black ovals (**A**) and quantified in **B** ($n = 6$ per group). **C–F**: Immunoblotting in measuring protein content of PGC-1 α (**D**), CYTO-C (**E**), and VDAC (**F**) in sorted brown progenitors in offspring BAT ($n = 6$ per group). β -Tubulin was used as a loading control. **G**: mtDNA copy of brown progenitors isolated in offspring BAT. Amplification of mitochondrial genes was standardized to 18S rRNA and GAPDH. $n = 6$ per group. **H** and **I**: Immunostaining (**H**) and fluorophore intensity (**I**) of mitochondria (Mito) in sorted brown progenitors using MitoSpy (green). Scale bars, 100 μm . **J–L**: Cell proliferation of brown progenitors was measured using MTT and BrdU assays. Progenitor cells were treated with BrdU for 24 h followed by BrdU and DAPI immunostaining (**K**); scale bars, 200 μm . Proliferative cells were displayed as BrdU $^+$ cells (**L**). **M** and **N**: Brown progenitors isolated from offspring BAT were induced into brown adipocytes using standard brown adipogenic differentiation protocol in vitro followed by lipid staining (**M**) and quantification (**N**) using oil red O ($n = 4$ per group). Data are means \pm SEM, and each dot represents one replicate (litter). * $P < 0.05$, ** $P < 0.01$, *** $P < 0.001$, **** $P < 0.0001$; unpaired Student t test with two-tailed distribution was used in analyses. APC, allophycocyanin; A.U., arbitrary units; CON, control; PE, phycoerythrin; Rel., relative.

to maternal DEX exposure (Fig. 2F). Taken together, these data showed that maternal hyper-GC impaired offspring BAT energy expenditure and thermogenesis, contributing to metabolic dysfunctions and cold intolerance in adult offspring.

Maternal GC Impairs Mitochondrial Biogenesis in BAT of Adult Offspring

Due to the importance of mitochondria in mediating thermogenesis and energy expenditure (15,16), we further analyzed mitochondrial density and structure in offspring BAT and found that brown adipocytes had larger sizes of lipid droplets but reduced mitochondria number and cristae length and density in DEX offspring fed with both chow and HFD (Fig. 3A–E). Consistent with the reduced

mitochondria number, BAT of DEX offspring also showed substantial decreases of mtDNA content (Fig. 3F) and mitochondrial biomass indicators VDAC and CYTO-C (Fig. 3G and Supplementary Fig. 4D and E). PGC-1 α centrally regulates mitochondrial biogenesis and UCP-1 thermogenesis, which was also profoundly reduced in DEX offspring BAT (Fig. 3G and H and Supplementary Fig. 4F), in alignment with the reduced expression of mitochondrial biogenic nuclear genes (Fig. 3I). Moreover, mitochondrial encoding genes involved in oxidative phosphorylation and respiration chain were also reduced in DEX offspring (Fig. 3I), showing that maternal GC exposure impaired *Pparg1a* expression and mitochondrial biogenesis in offspring BAT.

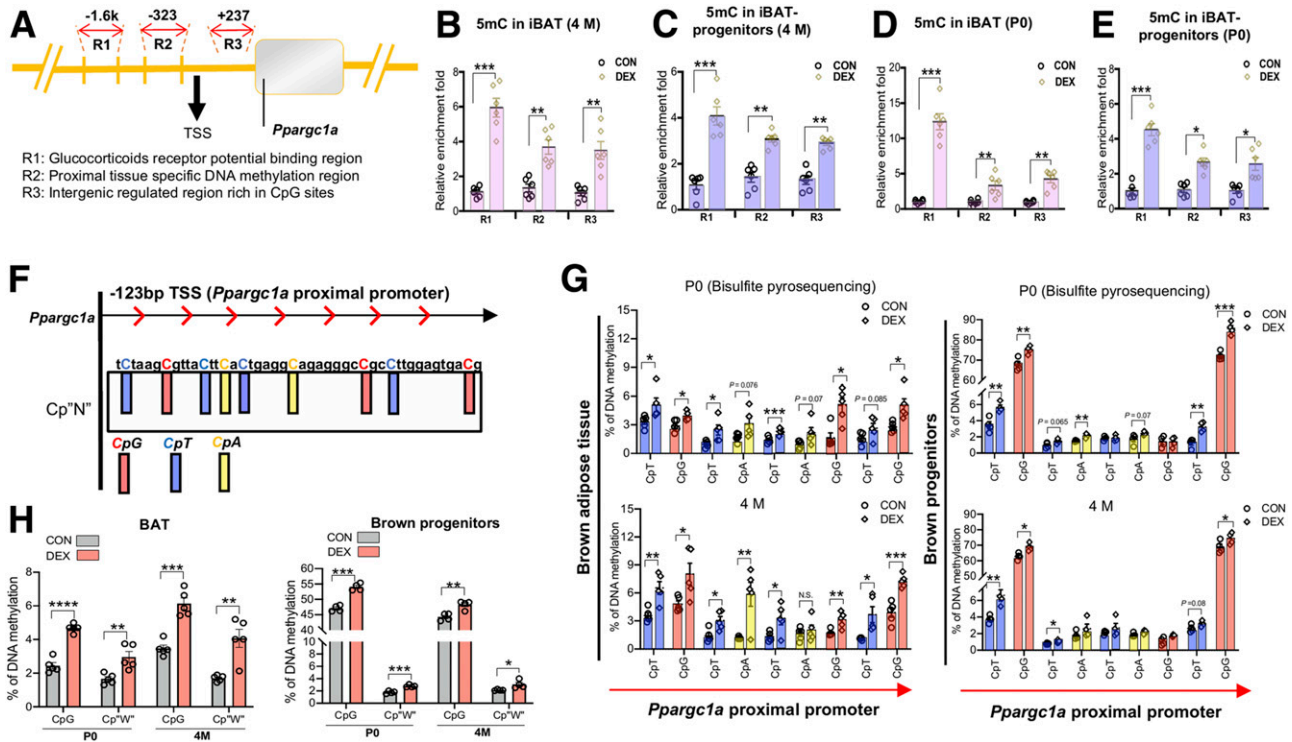


Figure 5—Maternal DEX administration increases DNA methylations in the *Pparg1a* promoter, which has a fetal origin and inhibits *Pparg1a* transcriptional activity in offspring BAT and brown progenitors. *A*: Diagram shows *Pparg1a* promoter and transcriptional starting site (TSS) shores, including a potential binding region (R) of GR (GRBR, R1), proximal tissue specific-DNA methylation region (T-DMR, R2), and intergenic regulated region rich in CpG sites (IR, R3). *B–E*: Relative fold changes of 5mC quantified by MeDIP qPCR in methylated regulatory regions R1, R2, and R3 of the *Pparg1a* promoter in BAT and sorted brown progenitors in offspring at 4 months of age (4 M) (*B* and *C*) and neonates at P0 (*D* and *E*). Mock IgG was used as a negative control. *F*: Diagram shows bisulfite pyrosequencing covering cytosine sites in the proximal promoter region of *Pparg1a*. *G*: Methylation content of individual cytosine in the sequenced *Pparg1a* proximal promoter in BAT and brown progenitors at P0 and 4 months old in offspring. *H*: Averaged cytosine methylation in CpG and CpW (A and T). $n = 6$ in each group. Data are means \pm SEM, and each dot represents one replicate (litter). * $P < 0.05$, ** $P < 0.01$, *** $P < 0.001$, **** $P < 0.0001$; unpaired Student t test with two-tailed distribution was used in analyses.

Maternal GC Suppresses Mitochondrial Biogenesis in Brown Progenitors of Adult Offspring

Because brown progenitors are responsible for BAT plasticity, we further isolated BAT stromal vascular cells and sorted for brown progenitors using well-characterized surface markers $Lin^- CD45^- /PDGFRa^+$ by FACS (32,33). BAT of DEX offspring had profoundly reduced brown progenitor density (Fig. 4A and B). Brown progenitors of DEX offspring also had the lower *Pparg1a* expression (Fig. 4C and D) and mitochondrial biomass as indicated by CYTO-C, VDAC, and mtDNA contents (Fig. 4C and E–G). Immunostaining using mitochondrial tracker robustly displayed lower mitochondrial density (Fig. 4H and I), verifying that the brown progenitors of DEX offspring had reduced capacity of mitochondrial biogenesis; progenitor plasticity is required for maintaining BAT thermogenic activation in responses to cold and other stimuli (33–35). In addition, isolated brown progenitors in DEX offspring BAT had reduced NAD(P)H-dependent oxidoreductase enzyme activity in MTT assay (Fig. 4J), and less incorporation of thymidine analog BrdU into nuclear DNA (Fig. 4K and L), suggesting lower proliferative capacity. Following a standard brown adipogenic induction, brown progenitors

of DEX offspring also displayed a reduced capacity to differentiate into brown adipocytes based on oil red O staining (Fig. 4M and N). Taken together, our data showed that maternal GC exposure decreased *Pparg1a* expression, mitochondrial biogenesis, and brown adipogenesis of progenitors in offspring BAT.

Maternal GC Increases DNA Methylation in *Pparg1a* Promoter, Which Has a Fetal Origin

Pparg1a is a master regulator of mitochondrial biogenesis, which was inhibited in BAT and brown progenitors in DEX offspring. We hypothesized that such inhibition was due to DNA methylation in the *Pparg1a* promoter, which is known to regulate its expression (18,19). Indeed, we noticed the proximal promoter of *Pparg1a* harbors CpG and noncanonical CpG methylation sites (Fig. 5A and Supplementary Fig. 5A). To analyze, we used MeDIP analysis and found that 5mC was higher in the *Pparg1a* promoter in both BAT and brown progenitors of DEX offspring at 4 months of age compared with control offspring (Fig. 5B and C). Intriguingly, the elevated DNA methylation was also observed in BAT and brown progenitors of DEX offspring at weaning (Supplementary Fig. 5B

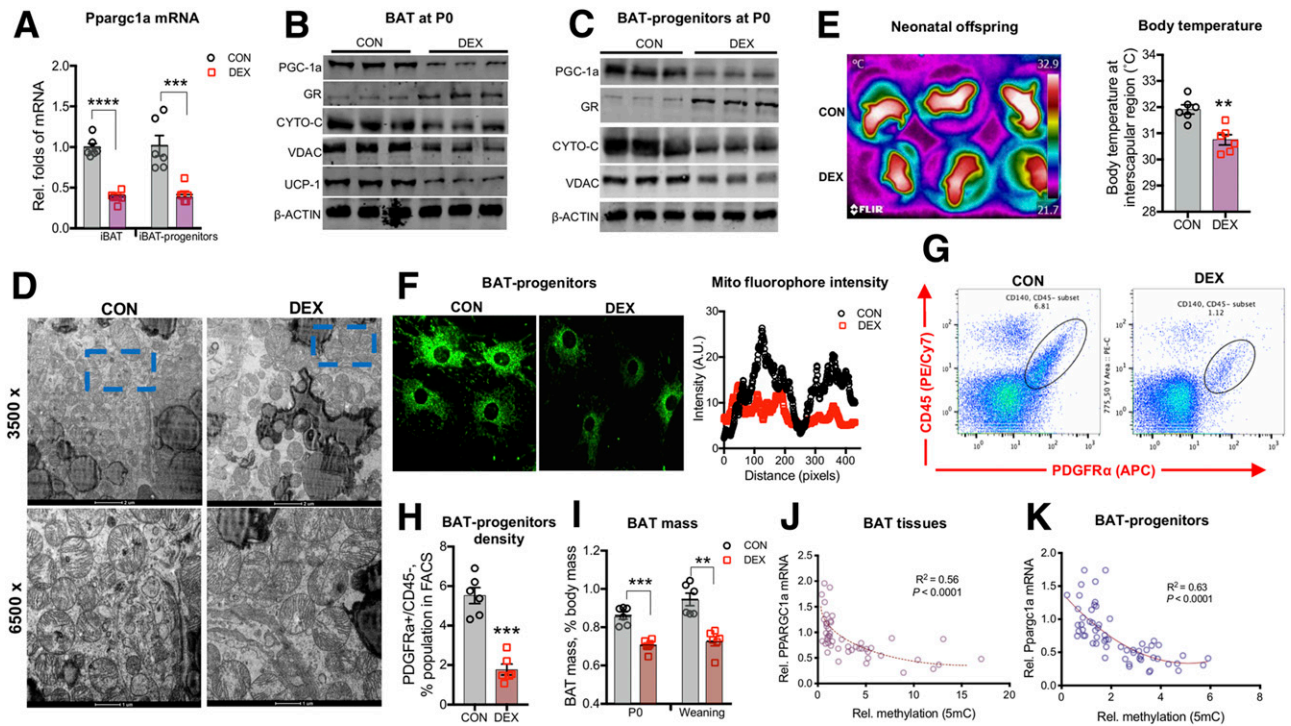


Figure 6—Maternal DEX inhibits *Ppargc1a* expression and mitochondrial biogenesis in fetal BAT and brown progenitors. *A–C*: After birth (P0), neonatal BAT and brown progenitors isolated from BAT were used for measurement of *Ppargc1a* mRNA (*A*) and protein contents of PGC-1 α , GR, CYTO-C, VDAC, and UCP-1 (*B* and *C*). mRNA expression was standardized to 18S rRNA, and β -actin was used as a loading control in Western blot. *D*: TEM imaging displayed mitochondrial density in neonatal BAT (scale bar, $\times 3,500$ for 2 μ m, $\times 6,500$ for 1 μ m). *E*: Thermal imaging of the surface temperature in the interscapular region of neonates at P0 ($n = 6$ per group). Measurements were performed immediately after neonates were separated from the nests in order to avoid heat loss at room temperature. *F*: Immunostaining and intensity of mitochondria (Mito) in brown progenitors sorted from neonatal BAT. MitoSpy (green) was used as a mitochondrial tracker. *G* and *H*: FACS for measuring the population of brown progenitors in neonatal BAT using progenitor markers: Lin⁻ CD45⁻/PDGFR α ⁺. Positive population of brown progenitors shown in black ovals (*G*) and quantified in *H* ($n = 6$ per group). *I*: BAT mass (% body mass) in neonates at P0 and offspring at weaning P21 ($n = 6$ per group). *J* and *K*: Correlation between 5mC abundance and mRNA expression of *Ppargc1a* in offspring BAT (*J*) and brown progenitors (*K*). Statistical analyses were assessed by linear and higher-order nonlinear regressions, respectively, and Bayesian information criterion was used for model selection among a finite set of regressions. With use of random Legendre regression analyses, second-degree polynomial regression model identified a higher prediction likelihood R^2 . Data are means \pm SEM, and each dot represents one replicate (litter). * $P < 0.05$, ** $P < 0.01$, *** $P < 0.001$, **** $P < 0.0001$; unpaired Student *t* test with two-tailed distribution was used in analyses. APC, allophycocyanin; A.U., arbitrary units; CON, control; iBAT, intrascapular BAT; Rel., relative.

and *C*) and further traced back to neonates at P0 (Fig. 5*D* and *E*), showing that higher DNA methylation in the *Ppargc1a* promoter of DEX offspring BAT had a fetal origin. However, DNA hypermethylations were not observed in the promoters of unrelated genes in BAT and brown progenitors of DEX neonates, including *Nrf1*, *Pax3*, and *Zfp423* (Supplementary Fig. 5*D* and *E*), suggesting locus-specific DNA methylation in gene promoters.

To identify methylation sites in the *Ppargc1a* proximal promoter, bisulfite pyrosequencing was performed (19,29) (Fig. 5*F*). BAT of DEX offspring did not only display higher methylation of CpG sites; intriguingly, hypermethylation was also observed in non-CpG sites (Fig. 5*G* and *H*). Similar patterns were also revealed from brown progenitors in DEX offspring (Fig. 5*G* and *H*), further highlighting that non-CpG methylation was likely involved in the regulation of *Ppargc1a* transcriptional activity.

In alignment with the higher DNA methylation in the *Ppargc1a* promoter, *Ppargc1a* expression was also profoundly lower in BAT and brown progenitors of DEX

neonates (Fig. 6*A–C*). In agreement, BAT of DEX neonates had elevated GR expression but reduced contents of UCP-1, VDAC, and CYTO-C, as well as mitochondria number and cristae density (Fig. 6*B–D* and Supplementary Fig. 6*A* and *B*). Consistent with GR activation in BAT, neonates displayed higher concentration of corticosterone, which was further confirmed in offspring at 4 months of age as assessed by GC suppression test (Supplementary Fig. 6*C*). Considering the critical role of neonatal BAT in maintaining body temperature, the reduced BAT thermogenesis explained the hypothermia in DEX neonates (Fig. 6*E*), which correlated with reduced survival of offspring in the first postnatal week (Supplementary Fig. 6*D*). Brown progenitors isolated from DEX neonates also had lower contents of mitochondrial biomass protein markers, mitochondrial density, and mtDNA (Fig. 6*C* and *F* and Supplementary Fig. 6*E*). Consistently, the population of brown progenitors was also reduced in DEX neonatal BAT (Fig. 6*G* and *H*). Furthermore, the brown progenitors had reduced capacity undergoing brown adipogenic

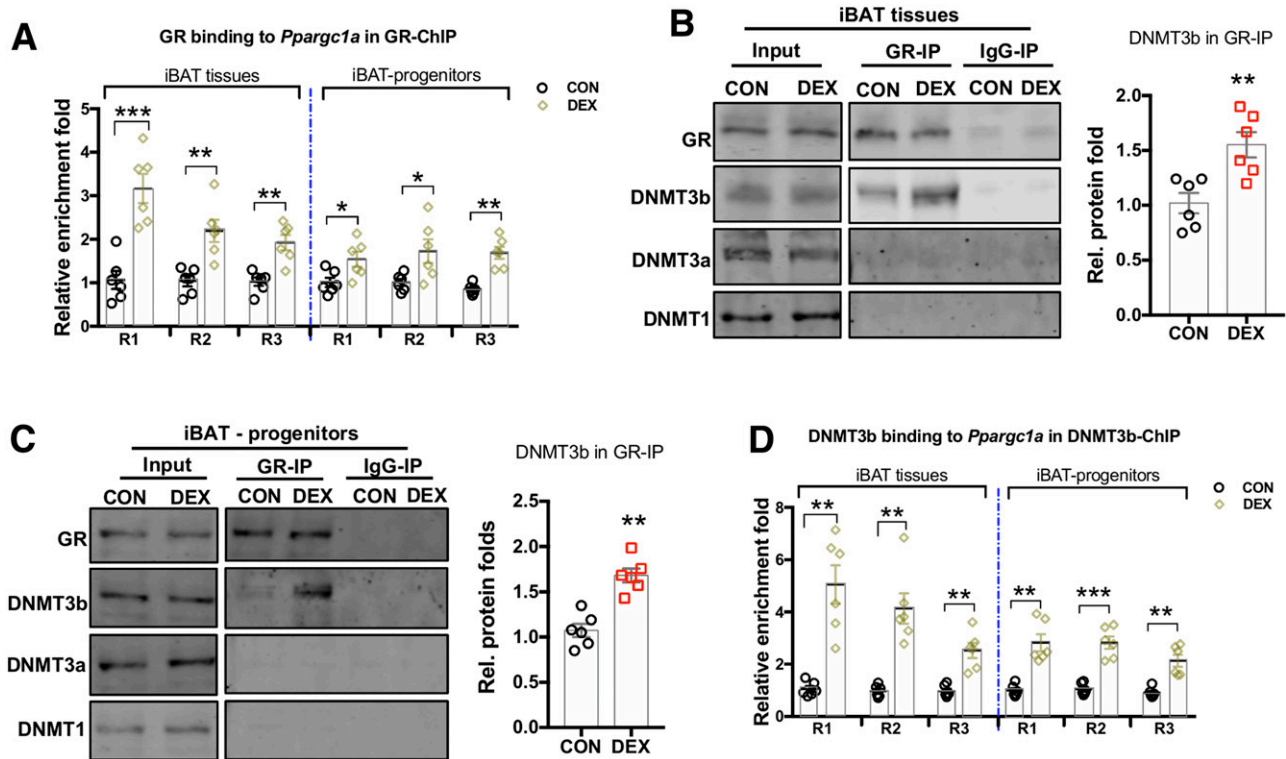


Figure 7—Maternal DEX increases the formation of GR and DNMT3b complex in binding to the *Ppargc1a* promoter in BAT and brown progenitors of fetus. **A**: Relative fold changes of GR abundance binding to *Ppargc1a* promoter and transcriptional starting site shores, including GR potential binding region (GRBR, region R1), proximal tissue specific-DNA methylation region (T-DMR, R2), and intergenic regulated region rich in CpG sites (IR, R3). Analyses were quantified using GR ChIP qPCR (GR-ChIP) in the *Ppargc1a* promoter region R1, R2, and R3 in BAT and brown progenitors of neonates at P0. Mock IgG was used as a negative control ($n = 6$ in each group). **B** and **C**: Coimmunoprecipitation of GR in neonatal BAT (**B**) and sorted brown progenitors (**C**). GR, DNMT3b, DNMT3a and DNMT1 were immunoprecipitated followed with SDS-PAGE separation and measured in Western blot. IgG was used as a negative control in immunoprecipitation ($n = 6$). **D**: Relative fold changes of DNMT3b binding to the *Ppargc1a* promoter and transcriptional starting site shores, including GR potential binding region (GRBR, R1), proximal tissue specific-DNA methylation region (T-DMR, R2), and intergenic regulated region rich in CpG sites (IR, R3) in BAT and brown progenitors of neonates at P0. Analyses were quantified by DNMT3b ChIP qPCR (DNMT3b-ChIP) in the *Ppargc1a* transcriptional regulatory regions in BAT and brown progenitors of neonates at P0. Mock IgG was used as a negative control ($n = 6$ in each group). Data are means \pm SEM, and each dot represents one replicate (litter). * $P < 0.05$, ** $P < 0.01$, *** $P < 0.001$; unpaired Student t test with two-tailed distribution was used in analyses. CON, control; iBAT, intrascapular BAT; IP, immunoprecipitation; R, region; Rel., relative.

differentiation in vitro (Supplementary Fig. 6F), supporting the suppressed BAT mass in DEX neonates (Fig. 6I). Similar data regarding to the *Ppargc1a* transcriptional inactivation and reduced BAT mitochondrial biogenesis and thermogenesis were also observed in DEX offspring at weaning (Supplementary Fig. 7A–H). Collectively, the DNA methylation of *Ppargc1a* promoter was inversely correlated with transcriptions in both BAT and brown progenitors in offspring (Fig. 6J and K). These data support the notion that the reduced *Ppargc1a* expression resulted from the abnormal gaining of DNA methylation in the *Ppargc1a* promoter during fetal BAT development of DEX mothers.

GR/DNMT3b Complex Potentially Mediates *Ppargc1a* Silencing During Fetal BAT Development

To identify the underlying mechanisms leading to the locus-specific increase in DNA methylation of *Ppargc1a* promoter, we analyzed DNA binding elements and

identified a potential GR-responsive binding element as previously described (36,37) (Supplementary Fig. 5A). Using GR ChIP analyses, we observed that the maternal DEX exposure increased GR binding to the *Ppargc1a* promoter in both neonatal BAT and brown progenitors (Fig. 7A). In GR coimmunoprecipitation analyses, DNMT3b, but neither DNMT3a nor DNMT1, physically interacted with GR (Fig. 7B and C). Accordingly, maternal GC exposure enhanced the interaction between GR and DNMT3b (Fig. 7B and C), suggesting that GR might increase the recruitment of DNMT3b into the *Ppargc1a* promoter for de novo DNA methylation in BAT and brown progenitors. Using DNMT3b ChIP analyses, we confirmed that the DEX administration increased DNMT3b binding to the *Ppargc1a* promoter in both BAT and brown progenitors (Fig. 7D). Increased GR interaction with DNMT3b was also observed in BAT of DEX offspring at 4 months of age (Supplementary Fig. 7I). Taken together, these data showed that *Ppargc1a*, as a GR target gene, was

subjected to the enhanced DNA methylation in its promoter during fetal BAT development, potentially involving the recruitment of the GR/DNMT3b complex to the *Ppargc1a* promoter, which persistently suppresses its expression and impairs mitochondrial biogenesis and fetal BAT development, programming postnatal offspring to metabolic dysfunctions.

DISCUSSION

The intrauterine environment has profound effects on fetal development and birth outcome, which can program metabolic health of offspring, including obesity and type 2 diabetes (4,8–11,38). Antenatal stress, depression, and preterm delivery are prevalent in women during pregnancy, leading to fetal exposure to substantial levels of GC in the uterus (6,7). Maternal stress and antenatal GC administration are associated with outcomes of low birth weight (39–42), which is also a strong indicator for obesity and type 2 diabetes risks (43), but mechanisms of maternal hyper-GC linking to offspring obesity remain poorly understood. The present findings represent, to our best knowledge, the first report that the maternal GC exposure during pregnancy impaired offspring BAT thermogenesis, which was correlated with glucose and insulin resistance, obesity, and cold sensitivity. The finding highlighted the importance of maintaining maternal psychological health and discretion using exogenous GC during pregnancy in order to protect offspring from metabolic dysfunctions (3). Mechanistically, our study also disclosed that the maternal GC exposure persistently inhibited *Ppargc1a* expression in BAT and brown progenitors, leading to impaired mitochondrial biogenesis (15,16). We also found that DEX elicited excessive DNA methylation in both canonical and noncanonical CpG sites in the *Ppargc1a* proximal promoter (19). Furthermore, the DNMT3b and GR complex was identified to mediate the accretion of DNA methylation in the *Ppargc1a* promoter during fetal BAT development. The discovery provides a potential target to reduce the risks of obesity and metabolic dysfunctions in offspring born from mothers who suffered from hyper-GC conditions.

In this study, we administered pregnant mice with 100 $\mu\text{g}/\text{kg}$ DEX in the third trimester, which was in the range of GC concentrations in maternal circulation under stress or during preterm delivering as previously described (44,45). This dose was >10-fold lower than the DEX administration in nonpregnant mice for anti-inflammatory therapy or pathological GC secretion in patients with an adrenal tumor such as in Cushing syndrome (46). The low dose and a relatively short duration of treatment might explain the lack of difference in food intake and body weight of maternal mice between treatments. However, we observed a profound GR activation in both BAT and brown progenitors of DEX neonates, suggesting that the low dose is sufficient to induce corresponding changes in fetuses. Therapeutic DEX administration to mothers

with preterm delivery improves lung maturation of fetuses, but it also increases risks of low birth weight (40,41). As for programming effects, under HFD, adult DEX offspring displayed insulin resistance, impaired glucose and fatty acid oxidization, and adiposity (8,14). Notably, DEX offspring fed with a normal calorie diet also displayed metabolic dysfunctions and adiposity, showing the negative effects of maternal hyper-GC on offspring health regardless of postnatal diets. For validation of the mediatory roles of BAT thermogenesis in reducing energy expenditure of DEX offspring at room temperature, adult offspring were also acclimated to thermoneutrality and exposed to acute cold, respectively (26–28). Under thermoneutrality, the reduction of energy expenditure in DEX offspring was substantially blunted. Meanwhile, DEX adult offspring, regardless of postweaning diet, displayed severe cold sensitivity and reduced brown thermogenesis under acute cold challenge, demonstrating that maternal hyper-GC exposure significantly impaired offspring BAT thermogenic activity, which mediated reduced energy expenditure and metabolic dysfunctions of their offspring. Of note, physical activity was not directly measured in offspring; thus, the potential effects of physical activity on offspring energy expenditure could not be excluded. On the other hand, we observed lower metabolic rates of DEX offspring during both nighttime (physically active) and daytime (inactive), suggesting physical activity was not a major factor contributing to metabolic dysfunction in DEX offspring.

Through regulating mitochondrial biogenesis, PGC-1 α transduces a variety of cellular functions (15,16), facilitating differentiation of progenitors and stem cells (34,35). Mitochondrial biogenesis activates energy expenditure and heat production of brown adipocytes (12). Sufficient energy provided from tricarboxylic cycle is also required for the biosynthetic platform during proliferation and differentiation of progenitors (47). In the absence or limitation of mitochondrial biogenesis, the proliferation and differentiation of progenitors are not sustained, suppressing tissue growth and regeneration (47). Maternal GC exposure reduced *Ppargc1a* expression in BAT of adult offspring, impairing mitochondrial biogenesis and thermogenesis. The detrimental effects were further observed in the sorted brown progenitors with use of well-characterized markers (32,33), explaining impaired BAT plasticity under cold stimulation. Brown progenitors are essential for BAT plasticity in response to environmental stimuli, including hormones and cold (13,33). Intriguingly, the impaired mitochondrial biogenesis and *Ppargc1a* transcription were further traced back to neonates. The neonatal offspring born from DEX dams displayed hypothermia and reduced BAT mass and thermogenic activity. The BAT thermogenic inactivation increases postnatal death in response to severe cold (12). Collectively, we revealed that maternal hyper-GC impaired fetal BAT development, which had persistent effects in impairing offspring BAT thermogenic function and plasticity.

Epigenetic regulation during fetal development exerts long-term programming impacts on gene expression, which may shape tissue developmental trajectory and lifelong health of offspring (4). We identified that BAT and brown progenitors of DEX offspring had higher DNA methylation in the *Ppargc1a* promoter. In the meantime, the hypermethylation was also observed in non-CpG sites, supporting a previous report that noncanonical CpG methylation may play a critical role in pathogenic *Ppargc1a* inactivation in patients with diabetes (19). The DNA methylations in the *Ppargc1a* promoter durably suppress *Ppargc1a* expression and mitochondrial biogenesis (18,19). Excessive DNA methylation in the *Ppargc1a* promoter was also reported in the muscle of patients with diabetes, causing impaired mitochondrial biogenesis and muscle atrophy (19). In this study, we also noticed the hyper-DNA methylation of *Ppargc1a* promoter in the muscle of DEX offspring (data not shown). As the energy expenditures in muscle and BAT are highly dependent on mitochondrial biogenesis, the *Ppargc1a* promoter methylation contributes to the pathogenesis of obesity and type 2 diabetes (18,19). Maternal hyper-GC exposure also programmed offspring hypothalamic-pituitary-adrenal axis as indicated by high cortisol in circulation and in response to GR activation, which might contribute to gaining of DNA methylation from elevated interaction between GR and DNMT3b in offspring BAT and brown progenitors (22). A similar interaction was also reported in neurons (48,49). Taken together, results indicate that the GC exposure enhanced the GR binding to the regulatory region of the *Ppargc1a* promoter, likely serving as a dock for DNMT3b recruitment, locally driving the de novo DNA methylation in the transcriptional regulatory regions of corresponding genes (48,49). These findings deepen our mechanistic understanding of maternal hyper-GC exposure in reducing energy expenditure and increasing susceptibility to metabolic dysfunctions of offspring (19). Of note, in this study, we only examined male offspring. Because the negative effects of excessive GC exposure during pregnancy have been well-documented to predispose offspring to obesity and metabolic dysfunctions in both sexes of mice and humans (8–11), biological changes identified in male offspring should be applicable to females.

In conclusion, we discovered that the maternal hyper-GC exposure during pregnancy substantially inhibits fetal BAT development, which was associated with persistent elevation of DNA methylation in the *Ppargc1a* promoter and increased risks of obesity and metabolic dysfunctions in offspring. These findings underscored that the prevalent maternal physiological stress or pharmacologic GC administration during pregnancy impaired metabolic health of offspring, which may contribute to the obesity epidemics in the modern society.

Acknowledgments. The authors thank Franceschi Microscopy & Imaging Center for help with electronic microscopy imaging.

Funding. This work was funded by the National Institutes of Health (NIH R01-HD067449).

Duality of Interest. No potential conflicts of interest relevant to this article were reported.

Author Contributions. Y.-T.C. and M.D. developed the concept, designed experiments, and interpreted the data. Y.-T.C., Y.H., J.S.S., X.-D.L., and J.M.d.A. conducted experiments and collected data. Y.-T.C., Y.H., and Q.-Y.Y. analyzed data. Y.-T.C. and M.D. prepared the manuscript. Y.-T.C., M.-J.Z., and M.D. made revisions to the manuscript. All authors approved the final content. Y.-T.C. and M.D. are the guarantors of this work and, as such, had full access to all the data in the study and take responsibility for the integrity of the data and the accuracy of the data analysis.

References

- Dennis CL, Falah-Hassani K, Shiri R. Prevalence of antenatal and postnatal anxiety: systematic review and meta-analysis. *Br J Psychiatry* 2017;210:315–323
- Bennett HA, Einarson A, Taddio A, Koren G, Einarson TR. Prevalence of depression during pregnancy: systematic review. *Obstet Gynecol* 2004;103:698–709
- McGowan PO, Matthews SG. Prenatal stress, glucocorticoids, and developmental programming of the stress response. *Endocrinology* 2018;159:69–82
- Cartier J, Smith T, Thomson JP, et al. Investigation into the role of the germline epigenome in the transmission of glucocorticoid-programmed effects across generations. *Genome Biol* 2018;19:50
- Mairesse J, Lesage J, Breton C, et al. Maternal stress alters endocrine function of the fetoplacental unit in rats. *Am J Physiol Endocrinol Metab* 2007;292:E1526–E1533
- Gitau R, Fisk NM, Glover V. Human fetal and maternal corticotrophin releasing hormone responses to acute stress. *Arch Dis Child Fetal Neonatal Ed* 2004;89:F29–F32
- Smith AK, Newport DJ, Ashe MP, et al. Predictors of neonatal hypothalamic-pituitary-adrenal axis activity at delivery. *Clin Endocrinol (Oxf)* 2011;75:90–95
- Entringer S, Wüst S, Kumsta R, et al. Prenatal psychosocial stress exposure is associated with insulin resistance in young adults. *Am J Obstet Gynecol* 2008;199:498.e1–498.e7
- Rondó PH, Ferreira RF, Nogueira F, Ribeiro MC, Lobert H, Artes R. Maternal psychological stress and distress as predictors of low birth weight, prematurity and intrauterine growth retardation. *Eur J Clin Nutr* 2003;57:266–272
- Drake AJ, Liu L, Kerrigan D, Meehan RR, Seckl JR. Multigenerational programming in the glucocorticoid programmed rat is associated with generation-specific and parent of origin effects. *Epigenetics* 2011;6:1334–1343
- Lindsay RS, Lindsay RM, Edwards CR, Seckl JR. Inhibition of 11-beta-hydroxysteroid dehydrogenase in pregnant rats and the programming of blood pressure in the offspring. *Hypertension* 1996;27:1200–1204
- Symonds ME. Brown adipose tissue growth and development. *Scientifica (Cairo)* 2013;2013:305763
- Harms M, Seale P. Brown and beige fat: development, function and therapeutic potential. *Nat Med* 2013;19:1252–1263
- Yang Q, Liang X, Sun X, et al. AMPK/α-ketoglutarate axis dynamically mediates DNA demethylation in the Prdm16 promoter and brown adipogenesis. *Cell Metab* 2016;24:542–554
- Fernandez-Marcos PJ, Auwerx J. Regulation of PGC-1α, a nodal regulator of mitochondrial biogenesis. *Am J Clin Nutr* 2011;93:884S–890S
- Uldry M, Yang W, St-Pierre J, Lin J, Seale P, Spiegelman BM. Complementary action of the PGC-1 coactivators in mitochondrial biogenesis and brown fat differentiation. *Cell Metab* 2006;3:333–341
- Semple RK, Crowley VC, Sewter CP, et al. Expression of the thermogenic nuclear hormone receptor coactivator PGC-1α is reduced in the adipose tissue of morbidly obese subjects. *Int J Obes Relat Metab Disord* 2004;28:176–179

18. Ling C, Del Guerra S, Lupi R, et al. Epigenetic regulation of PPARGC1A in human type 2 diabetic islets and effect on insulin secretion. *Diabetologia* 2008;51:615–622
19. Barrès R, Osler ME, Yan J, et al. Non-CpG methylation of the PGC-1alpha promoter through DNMT3B controls mitochondrial density. *Cell Metab* 2009;10:189–198
20. Luijten IHN, Cannon B, Nedergaard J. Glucocorticoids and brown adipose tissue: do glucocorticoids really inhibit thermogenesis? *Mol Aspects Med* 2019;68:42–59
21. Ramage LE, Akyol M, Fletcher AM, et al. Glucocorticoids acutely increase brown adipose tissue activity in humans, revealing species-specific differences in UCP-1 regulation. *Cell Metab* 2016;24:130–141
22. de Vries A, Holmes MC, Heijnen A, et al. Prenatal dexamethasone exposure induces changes in nonhuman primate offspring cardiometabolic and hypothalamic-pituitary-adrenal axis function. *J Clin Invest* 2007;117:1058–1067
23. Lim WL, Idris MM, Kevin FS, Soga T, Parhar IS. Maternal dexamethasone exposure alters synaptic inputs to gonadotropin-releasing hormone neurons in the early postnatal rat. *Front Endocrinol (Lausanne)* 2016;7:117
24. Huang LT. The link between perinatal glucocorticoids exposure and psychiatric disorders. *Pediatr Res* 2011;69:19R–25R
25. Leviton LC, Goldenberg RL, Baker CS, et al. Methods to encourage the use of antenatal corticosteroid therapy for fetal maturation: a randomized controlled trial. *JAMA* 1999;281:46–52
26. Riis-Vestergaard MJ, Breining P, Pedersen SB, et al. Evaluation of active brown adipose tissue by the use of hyperpolarized [1-¹³C]pyruvate MRI in mice. *Int J Mol Sci* 2018;19:2597
27. Galmozzi A, Kok BP, Kim AS, et al. PGRMC2 is an intracellular haem chaperone critical for adipocyte function. *Nature* 2019;576:138–142
28. Grimpo K, Völker MN, Heppe EN, Braun S, Heverhagen JT, Heldmaier G. Brown adipose tissue dynamics in wild-type and UCP1-knockout mice: in vivo insights with magnetic resonance. *J Lipid Res* 2014;55:398–409
29. Marshall MR, Paneth N, Gerlach JA, et al. Differential methylation of insulin-like growth factor 2 in offspring of physically active pregnant women. *J Dev Orig Health Dis* 2018;9:299–306
30. Tschöp MH, Speakman JR, Arch JRS, et al. A guide to analysis of mouse energy metabolism. *Nat Methods* 2011;9:57–63
31. Speakman JR. Measuring energy metabolism in the mouse - theoretical, practical, and analytical considerations. *Front Physiol* 2013;4:34
32. Schulz TJ, Huang TL, Tran TT, et al. Identification of inducible brown adipocyte progenitors residing in skeletal muscle and white fat. *Proc Natl Acad Sci U S A* 2011;108:143–148
33. Lee Y-H, Petkova AP, Mottillo EP, Granneman JG. In vivo identification of bipotential adipocyte progenitors recruited by β 3-adrenoceptor activation and high-fat feeding. *Cell Metab* 2012;15:480–491
34. Basu S, Broxmeyer HE, Hangoc G. Peroxisome proliferator-activated- γ coactivator-1 α -mediated mitochondrial biogenesis is important for hematopoietic recovery in response to stress. *Stem Cells Dev* 2013;22:1678–1692
35. Luo C, Widlund HR, Puigserver P. PGC-1 coactivators: shepherding the mitochondrial biogenesis of tumors. *Trends Cancer* 2016;2:619–631
36. So AY, Chaivorapol C, Bolton EC, Li H, Yamamoto KR. Determinants of cell- and gene-specific transcriptional regulation by the glucocorticoid receptor. *PLoS Genet* 2007;3:e94
37. Meijnsing SH, Pufall MA, So AY, Bates DL, Chen L, Yamamoto KR. DNA binding site sequence directs glucocorticoid receptor structure and activity. *Science* 2009;324:407–410
38. Neri C, Edlow AG. Effects of maternal obesity on fetal programming: molecular approaches. *Cold Spring Harb Perspect Med* 2015;6:a026591
39. Torche F. The effect of maternal stress on birth outcomes: exploiting a natural experiment. *Demography* 2011;48:1473–1491
40. French NP, Hagan R, Evans SF, Godfrey M, Newnham JP. Repeated antenatal corticosteroids: size at birth and subsequent development. *Am J Obstet Gynecol* 1999;180:114–121
41. Jensen EC, Gallaher BW, Breier BH, Harding JE. The effect of a chronic maternal cortisol infusion on the late-gestation fetal sheep. *J Endocrinol* 2002;174:27–36
42. Feldman PJ, Dunkel-Schetter C, Sandman CA, Wadhwa PD. Maternal social support predicts birth weight and fetal growth in human pregnancy. *Psychosom Med* 2000;62:715–725
43. Jornayvaz FR, Vollenweider P, Bochud M, Mooser V, Waeber G, Marques-Vidal P. Low birth weight leads to obesity, diabetes and increased leptin levels in adults: the CoLaus study. *Cardiovasc Diabetol* 2016;15:73
44. Agnew EJ, Garcia-Burgos A, Richardson RV, et al. Antenatal dexamethasone treatment transiently alters diastolic function in the mouse fetal heart. *J Endocrinol* 2019;241:279–292
45. Noorlander CW, Tijsseling D, Hessel EV, et al. Antenatal glucocorticoid treatment affects hippocampal development in mice. *PLoS One* 2014;9:e85671
46. Paragliola RM, Papi G, Pontecorvi A, Corsello SM. Treatment with synthetic glucocorticoids and the hypothalamus-pituitary-adrenal axis. *Int J Mol Sci* 2017;18:2201
47. DeBerardinis RJ, Lum JJ, Hatzivassiliou G, Thompson CB. The biology of cancer: metabolic reprogramming fuels cell growth and proliferation. *Cell Metab* 2008;7:11–20
48. Hervouet E, Peixoto P, Delage-Mourroux R, Boyer-Guittaut M, Cartron PF. Specific or not specific recruitment of DNMTs for DNA methylation, an epigenetic dilemma. *Clin Epigenetics* 2018;10:17
49. Sharma D, Bhave S, Gregg E, Uht R. Dexamethasone induces a putative repressor complex and chromatin modifications in the CRH promoter. *Mol Endocrinol* 2013;27:1142–1152